**Electronic supplementary information**

# Unexpected formation of a dodecanuclear $\{Co^{II}_6Cu^{II}_6\}$ nanowheel under ambient conditions: magneto-structural correlations

Walace D. do Pim,[a,b] Ingrid F. Silva,[a] Eufrânio N. da Silva Júnior,[a] Humberto O. Stumpf,[a] Willian X. C. Oliveira,[a] Emerson F. Pedroso,[b] Carlos B. Pinheiro,[c] Yves Journaux,[d] Felipe Fantuzzi,[e,f,g] Ivo Krummenacher,[f,g] Holger Braunschweig,[f,g] Bernd Engels,[e] Joan Cano,*[h] Miguel Julve,[h] and Cynthia L. M. Pereira*[a]

[a] Departamento de Química, Universidade Federal de Minas Gerais, Av. Antônio Carlos, 6627, Pampulha, Belo Horizonte, Minas Gerais, 31270-901, Brazil. E-mail: cynthialopes@ufmg.br

[b] Departamento de Química, Centro Federal de Educação Tecnológica de Minas Gerais Av. Amazonas, 5253, Belo Horizonte, MG, 30421-169, Brazil.

[c] Departamento de Física, Universidade Federal de Minas Gerais, Av. Antônio Carlos, 6627, Pampulha, Belo Horizonte, Minas Gerais, 31270-901, Brazil.

[d] Sorbonne Université, CNRS, Institut Parisien de Chimie Moléculaire, IPCM, 75252, Paris, France

[e] Institut für Physikalische und Theoretische Chemie, Julius Maximilians-Universität Würzburg, Emil-Fischer-Straße 42, 97074 Würzburg, Germany

[f] Institut für Anorganische Chemie, Julius Maximilians-Universität Würzburg, Am Hubland, 97074 Würzburg, Germany

[g] Institute for Sustainable Chemistry & Catalysis with Boron, Julius Maximilians-Universität Würzburg, Am Hubland, 97074 Würzburg, Germany

[h] Instituto de Ciencia Molecular/Departament de Química Inorgànica, Universitat de València, C/ Catedrático José Beltrán 2, 46980 Paterna, València, Spain. E-mail: joan.cano@uv.es

## Summary



**Figure S1.** FTIR spectra of $\{Co^{II}_6Cu^{II}_6\}$ and $K_2(H_2edpba)$ recorded using KBr pellets.

**Figure S2.** TG curve of $\{Co^{II}_6Cu^{II}_6\}$ obtained under synthetic air atmosphere.

**Figure S3.** Reduced magnetization curves of $\{Co^{II}_6Cu^{II}_6\}$ at the indicated temperatures. The solid lines are only eye-guides.

**Figure S4**. (a) Perspective drawing of the $\{Co^{II}_6Cu^{II}_6\}$ wheel without the Ph-$(CH_2)_2$-Ph ligand's moiety for a better view of the cyclic oxamate coordination. Thermal ellipsoids are drawn at the 25% probability level. Hydrogen atoms are omitted for clarity. Colour scheme for the non-labelled atoms: carbon (grey), oxygen (red) and nitrogen (sky blue). (b) A schematic representation of the metal atoms of the dodecanuclear $\{Co^{II}_6Cu^{II}_6\}$ wheel showcasing its twisted-boat conformation.

**Figure S5.** Reduced $\chi_M T$ *vs*. *T*/*J* plots as a function of the *D*/*J* quotient in the ranges (a) 0.0 to –2.0 and (b) –0.8 to –1.6. All curves were simulated considering $J = -50$ cm$^{-1}$.

**Figure S6.** Variable temperature X-band EPR spectra of the $\{Co^{II}_6Cu^{II}_6\}$ nanowheel between 4.0 and 40 K. The inset shows an expanded view of the low-field part of the spectrum. The signal around a *g* value of 2.05 could be due to trace amounts of some uncoupled mononuclear copper(II) ions.

**Table S1.** Crystal data and structure refinement parameters for $\{Co^{II}_6Cu^{II}_6\}$.

**Table S2.** Selected bond lengths (Å) and angles (deg) for $\{Co^{II}_6Cu^{II}_6\}$.

**Table S3.** Hydrogen bonds in $\{Co^{II}_6Cu^{II}_6\}$.

**Table S4.** Relevant structural parameters involved in the different magnetic exchange pathways of the $\{Co^{II}_6Cu^{II}_6\}$ nanowheel together with the more appropriate symmetry for each site and the $J_{i,j}$ values estimated from DFT calculations.

**Table S5.** Electronic energies (in hartrees) of the high-spin state ($S$ = 12) [*E(HS)*] and broken symmetry ($S$ = 6) [*E(BS)*] states of **1** obtained using distinct density functionals.

## 1. Experimental section

### 1.1. Materials and methods

All reactants used in this work were from analytical grade and they were used without further purification. The $Et_2H_2$edpba proligand and $(n\text{-}Bu_4N)_4[Cu_2(edpba)_2]\cdot 4H_2O$ precursor were synthesised according to the literature methods.[1] Elemental analysis (C, H and N) was performed with a Perkin-Elmer 2400 analyser. The contents of copper and cobalt were determined by atomic absorption spectroscopy with a Hitachi Z-8200 Polarised Atomic Absorption Spectrophotometer. Fourier transform infrared spectra (FTIR) were recorded with a Perkin-Elmer GX FTIR spectrophotometer in the range 4000-400 $cm^{-1}$ by using KBr pellets. Thermogravimetric analysis (TG) was carried out with a Shimadzu TG-60 thermal analyzer under synthetic air atmosphere (flow rate = 50 $cm^3\ min^{-1}$) at a heating rate of 10 °C $min^{-1}$ from room temperature to 900 °C. The d.c. magnetic susceptibility measurements were performed with a SQUID Cryogenic S600 magnetometer. The diamagnetic corrections for the constituent atoms were estimated from Pascal's tables.[2] Corrections for the temperature-independent paramagnetism [60 x $10^{-6}$ $cm^3\ mol^{-1}$ per copper(II) ion] as well as for the sample holder were also applied.

### 1.2. Synthesis of $[Co_6Cu_6(edpba)_6(H_2O)_{17}]\cdot 33H_2O$ – $\{Co^{II}_6Cu^{II}_6\}$

The $\{Co^{II}_6Cu^{II}_6\}$ nanowheel was obtained as follows: $(Bu_4N)_4[Cu_2(edpba)_2]\cdot 4H_2O$ (0.050 g, 0.03 mmol) dissolved in 1.0 mL of water was introduced in one arm of an H-shaped tube and $CoCl_2\cdot 6H_2O$ (0.030 g, 0.13 mmol) was deposited in the other one. The tube was carefully filled with water, capped with parafilm on both arms, and maintained at room temperature allowing for the diffusion of the starting materials. X-ray quality dark green prisms were formed after two weeks. Yield: 70%. Anal. Calcd for $C_{108}H_{172}Cu_6Co_6N_{12}O_{86}$: C, 34.60; H, 4.62; N, 4.48; Cu, 10.17; Co, 9.47. Found: C, 34.91; H, 4.61; N, 4.59; Cu, 10.50; Co, 9.71%. IR/$cm^{-1}$: 3412 [ν(O–H)], 1604 and 1583 [ν(C=O)], 1570 [ν(C=C)] and 1486, 1452 and 1344 [δ(–$CH_2$–)].

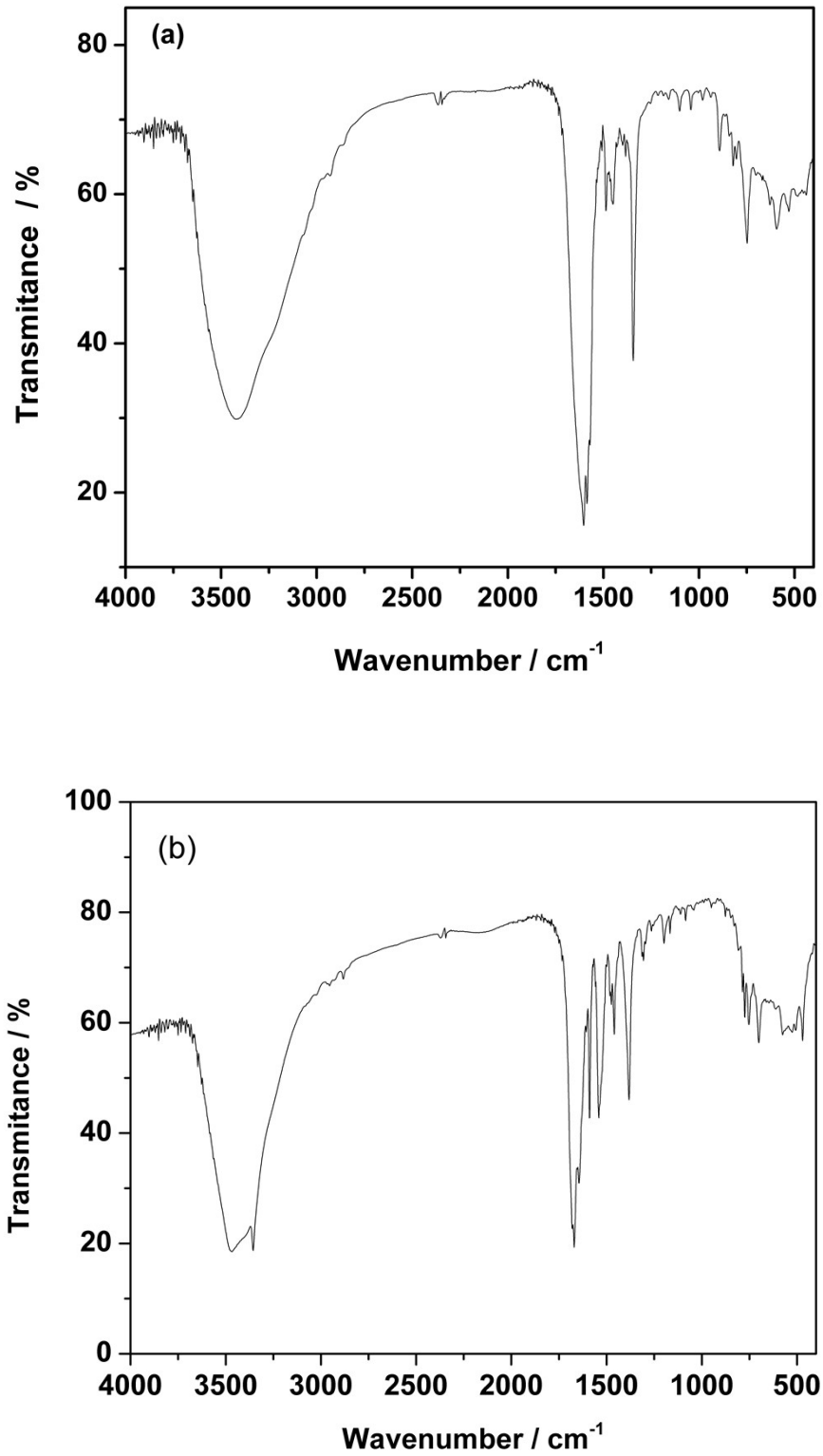


**Figure S1.** IR spectra of (a) $\{Co^{II}_6Cu^{II}_6\}$ and (b) $K_2(H_2edpba)$ recorded using KBr pellets.

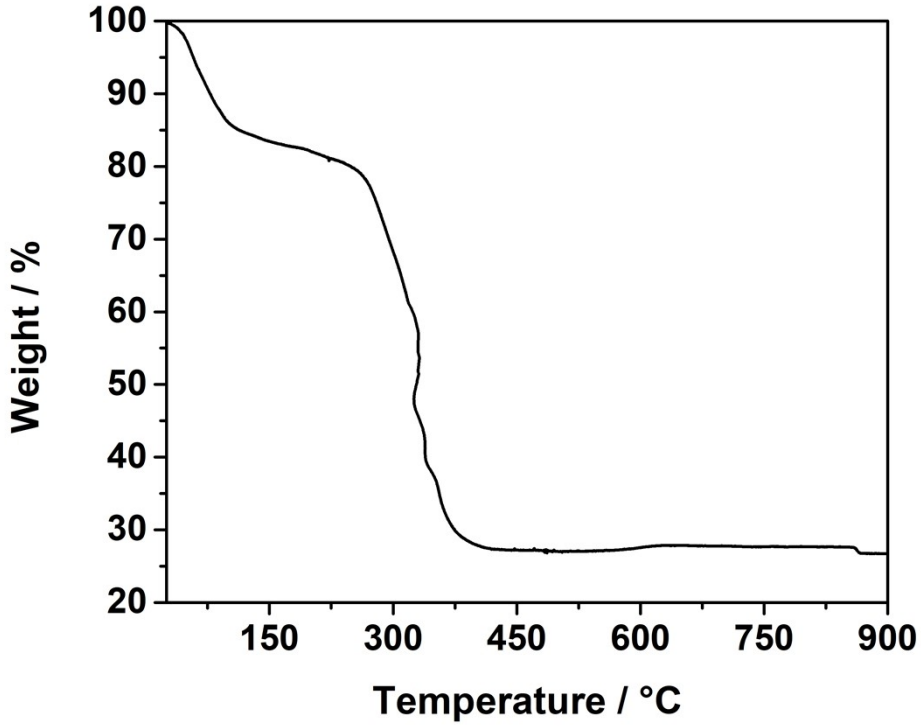


**Figure S2.** TG curve of $\{Co^{II}_6Cu^{II}_6\}$ obtained under synthetic air atmosphere.

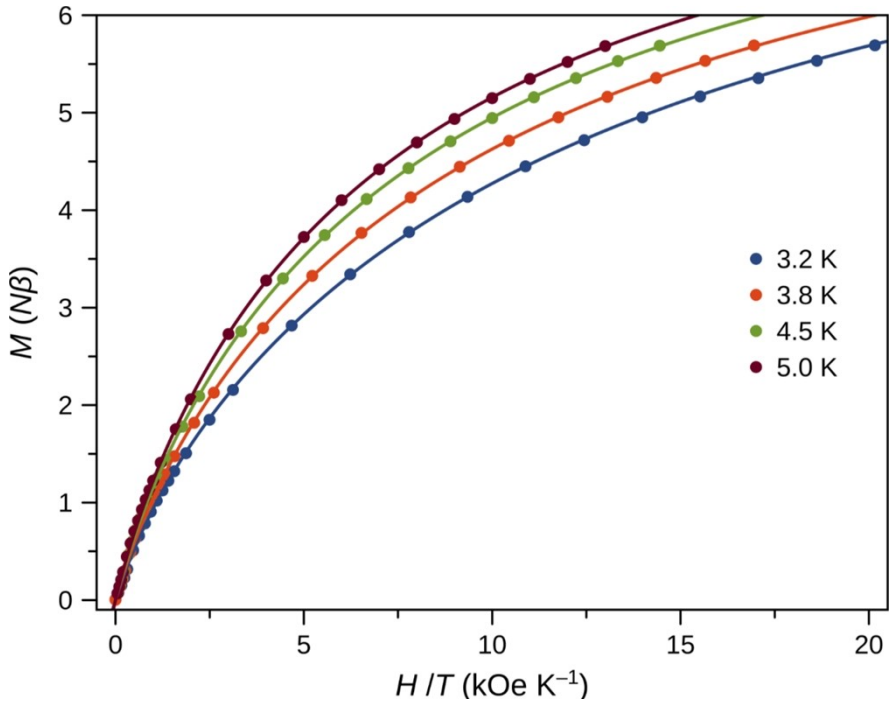


**Figure S3.** Reduced magnetisation curves of $\{Co^{II}_6Cu^{II}_6\}$ at the indicated temperatures. The solid lines are only eye-guides.

## 2. X-ray crystallography

X-ray diffraction data for $[Co_6Cu_6(edpba)_6(H_2O)_{17}]\cdot 33H_2O$ (**1**) was performed with an Oxford-Diffraction GEMINI-Ultra diffractometer using Enhance Source Cu-$K_\alpha$ radiation ($\lambda$ = 1.5418 Å). Data collection was performed at 110(2) K. Data integration and scaling of the reflections for **1** was carried out with the *Crysalis* suite of programs.[3] Final unit cell parameters are based on the fitting of all reflections positions. The space group and analytical[3] absorption corrections were performed using the *Crysalis* suite of programs. Identification is done with *XPREP*. The structure of **1** was solved *via* direct methods using the *SUPERFLIP* program.[4] The positions of $[Co_6Cu_6(edpba)_6(H_2O)_{17}]$ atoms could be unambiguously assigned on consecutive difference Fourier maps. Remarkably no electron density was identified at the apical positions near one of the copper atoms (Cu2). Refinement is performed by using *SHELXL*[5] based on $F^2$ through a full-matrix least-squares routine. All atoms except hydrogen and oxygen from water molecules were refined with anisotropic atomic displacement parameters. All hydrogen atoms were located in difference maps and included as fixed contributions according to the riding model.[6] C–H = 0.97 Å and $U_{iso}(H)$ = 1.2 $U_{eq}(C)$ for the methylene groups and aromatic carbon atoms of the organic moieties. O–H = 0.90 Å and $U_{iso}(H)$ = 1.5 $U_{eq}(O)$ for the water molecules. During the refinement, it was noticed some remarkable disordered water molecules of crystallisation in large voids in the structure of **1**. Thus, squeeze technique was applied using *PLATON* suite.[7] The procedure suppressed a total of 925 electrons in 2251 Å$^3$ per unit cell. Only water molecules of crystallization were masked in the processes. This result is compatible with the 34 water molecules (water electron density of 18e$^-$/30 Å$^3$) in the unit cell of **1**. Mercury program was used to prepare all crystal structure drawings.[8] The crystal data and structure refinements of **1** is listed in Table S1. Selected bond lengths and angles and hydrogen bonds are given in Tables 2 and 3, respectively. CCDC-1031229 contains the supplementary crystallographic data for this paper. These data can be obtained free of charge via www.ccdc.cam.ac.uk/conts/retrieving.html (or from the Cambridge Crystallographic Data Centre, 12, Union Road, Cambridge CB21EZ, UK; fax: (+44) 1223-336-033; or deposit@ccdc.cam.ac.uk).

**Table S1.** Crystal data and structure refinement parameters for $\{Co^{II}_6Cu^{II}_6\}$

| | **$\{Co^{II}_6Cu^{II}_6\}$** |
|---|---|
| Formula | $C_{108}H_{172}N_{12}Cu_6Co_6O_{86}$ |
| Formula weight | 3749.42 |
| Crystal size (mm) | 0.84 × 0.42 × 0.20 |
| Crystal System | Triclinic |
| Space group | $P\bar{1}$ |
| $T$ (K) | 110(2) |
| $a$ (Å) | 19.4553(11) |
| $b$ (Å) | 19.8342(11) |
| $c$ (Å) | 24.4381(10) |
| α (Å) | 66.283(4) |
| β (Å) | 85.356(4) |
| γ (Å) | 63.550(5) |
| $V$ (Å$^3$) | 7674.3(7) |
| $Z$ | 2 |
| $D_{calcd}$ (g cm$^{-3}$) | 1.579 |
| μ (mm$^{-1}$) | 6.494 |
| $F$(000) | 3169 |
| | |
| Total reflections collected [$R_{int}$] | 92705 [0.1354] |
| Independent reflections collected | 26825 |
| Independent reflections with $I \geq 2\sigma(I)$ | 14312 |
| Goodness-of-fit on $F^2$ ($S$) | 0.959 |
| $R^a$, $wR^b$ [$I > 2\sigma(I)$] | 0.1120/0.2828 |
| $R^a$, $wR^b$ (all data) | 0.1574/0.3152 |
| Larg. diff. peak and hole/e Å$^{-3}$) | 2.578/–0.753 |

$^aR = \Sigma||F_o|-|F_c||/\Sigma|F_o|$. $^bwR = [\Sigma(|F_0|^2-|F_c|^2)^2/\Sigma|F_o|^2]^{1/2}$.

(a)

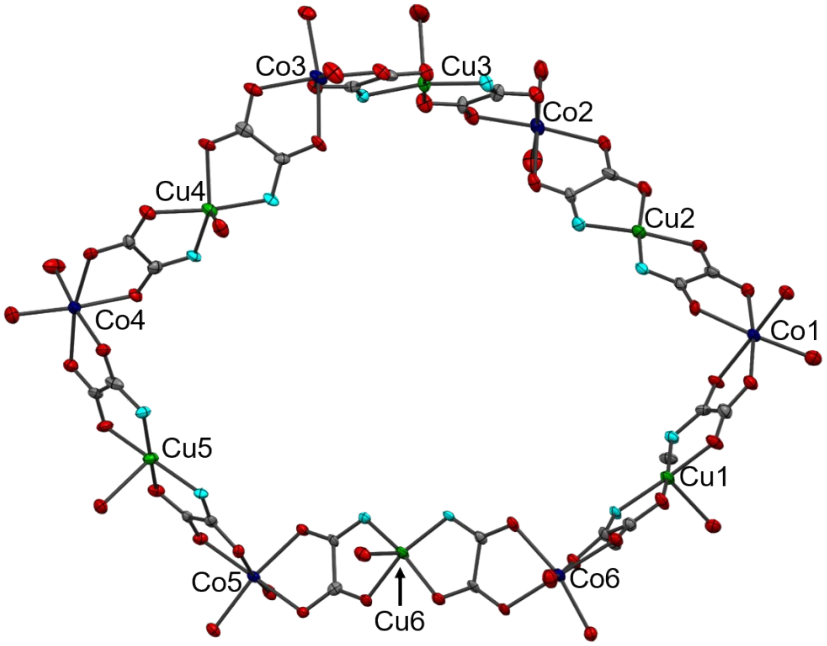


(b)

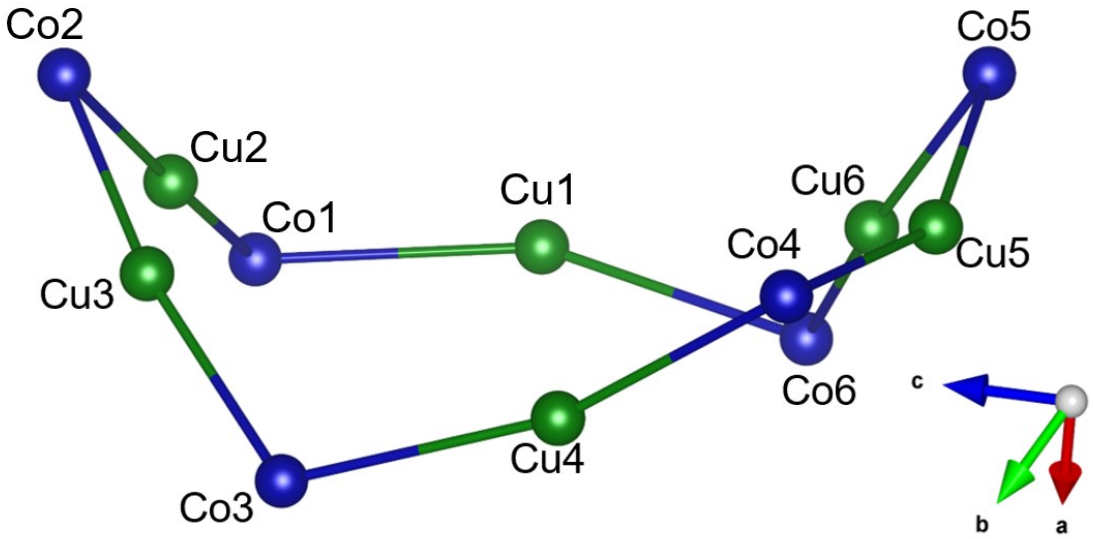


**Figure S4.** (a) Perspective drawing of the $\{Co^{II}_6Cu^{II}_6\}$ wheel without the Ph-$(CH_2)_2$-Ph ligand's moiety for a better view of the cyclic oxamate coordination. Thermal ellipsoids are drawn at the 25% probability level. Hydrogen atoms are omitted for clarity. Colour scheme for the non-labelled atoms: carbon (grey), oxygen (red) and nitrogen (sky blue). (b) A schematic representation of the metal atoms of the dodecanuclear $\{Co^{II}_6Cu^{II}_6\}$ wheel showcasing its twisted-boat conformation.

**Table S2.** Selected bond lengths (Å) and angles (deg) for $\{Co^{II}_6Cu^{II}_6\}$

| M–L | Bond length/Å | L–M–L | Bond angle/° | M–L | Bond length/Å | L–M–L | Bond angle/° |
|---|---|---|---|---|---|---|---|
| Cu1—N1 | 1.998 (8) | O1—Cu1—N13 | 168.3 (3) | Cu2—N2 | 1.951 (9) | N3—Cu2—N2 | 104.4 (4) |
| Cu1—N13 | 1.997 (7) | O1—Cu1—N1 | 82.9 (3) | Cu2—N3 | 1.929 (10) | N3—Cu2—O4 | 162.7 (4) |
| Cu1—O1 | 1.992 (7) | N13—Cu1—N1 | 105.5 (3) | Cu2—O4 | 1.960 (8) | N2—Cu2—O4 | 85.3 (3) |
| Cu1—O34 | 2.018 (8) | O1—Cu1—O34 | 85.7 (3) | Cu2—O7 | 1.989 (8) | N3—Cu2—O7 | 83.8 (4) |
| Cu1—O37 | 2.259 (8) | N13—Cu1—O34 | 84.1 (3) | | | N2—Cu2—O7 | 169.4 (3) |
| | | N1—Cu1—O34 | 161.9 (4) | | | O4—Cu2—O7 | 88.5 (3) |
| | | O1—Cu1—O37 | 92.7 (3) | | | | |
| | | N13—Cu1—O37 | 94.5 (3) | | | | |
| | | N1—Cu1—O37 | 95.0 (3) | | | | |
| | | O34—Cu1—O37 | 99.6 (3) | | | | |
| **M–L** | **Bond length/Å** | **L–M–L** | **Bond angle/°** | **M–L** | **Bond length/Å** | **L–M–L** | **Bond angle/°** |
| Cu3—N4 | 1.963 (9) | N4—Cu3—O13 | 94.4 (3) | Cu4—N6 | 1.981 (8) | N7—Cu4—N6 | 105.5 (3) |
| Cu3—N5 | 1.990 (8) | N4—Cu3—O10 | 83.6 (4) | Cu4—N7 | 1.974 (7) | N7—Cu4—O19 | 81.7 (3) |
| Cu3—O10 | 1.979 (7) | O13—Cu3—O10 | 172.6 (4) | Cu4—O16 | 2.059 (7) | N6—Cu4—O19 | 172.4 (3) |
| Cu3—O13 | 1.963 (7) | N4—Cu3—N5 | 169.4 (4) | Cu4—O19 | 1.989 (8) | N7—Cu4—O16 | 141.3 (3) |
| Cu3—O42 | 2.317 (10) | O13—Cu3—N5 | 85.2 (3) | Cu4—O45 | 2.196 (7) | N6—Cu4—O16 | 83.7 (3) |
| | | O10—Cu3—N5 | 95.4 (3) | | | O19—Cu4—O16 | 89.0 (3) |
| | | N4—Cu3—O42 | 91.1 (4) | | | N7—Cu4—O45 | 117.0 (3) |
| | | O13—Cu3—O42 | 96.8 (5) | | | N6—Cu4—O45 | 92.0 (3) |
| | | O10—Cu3—O42 | 90.4 (5) | | | O19—Cu4—O45 | 87.0 (3) |
| | | N5—Cu3—O42 | 99.5 (4) | | | O16—Cu4—O45 | 99.8 (3) |
| **M–L** | **Bond length/Å** | **L–M–L** | **Bond angle/°** | **M–L** | **Bond length/Å** | **L–M–L** | **Bond angle/°** |
| Cu5—N8 | 1.997 (8) | N8—Cu5—N9 | 107.5 (3) | Cu6—N10 | 2.009 (8) | O31—Cu6—O28 | 83.9 (3) |
| Cu5—N9 | 2.002 (8) | N8—Cu5—O22 | 83.0 (3) | Cu6—N11 | 1.981 (7) | O31—Cu6—N11 | 83.2 (3) |
| Cu5—O22 | 2.003 (8) | N9—Cu5—O22 | 167.3 (3) | Cu6—O28 | 1.979 (6) | O28—Cu6—N11 | 166.2 (3) |
| Cu5—O25 | 2.025 (6) | N8—Cu5—O25 | 162.5 (3) | Cu6—O31 | 1.967 (7) | O31—Cu6—N10 | 162.0 (3) |
| Cu5—O48 | 2.333 (7) | N9—Cu5—O25 | 85.3 (3) | Cu6—O53 | 2.332 (7) | O28—Cu6—N10 | 83.0 (3) |
| | | O22—Cu5—O25 | 83.0 (3) | | | N11—Cu6—N10 | 108.5 (3) |
| | | N8—Cu5—O48 | 98.1 (3) | | | O31—Cu6—O53 | 89.8 (3) |
| | | N9—Cu5—O48 | 94.3 (3) | | | O28—Cu6—O53 | 87.4 (3) |
| | | O22—Cu5—O48 | 91.1 (3) | | | N11—Cu6—O53 | 97.3 (3) |
| | | O25—Cu5—O48 | 92.7 (3) | | | N10—Cu6—O53 | 101.9 (3) |

| M–L | Bond length/Å | L–M–L | Bond angle/º | M–L | Bond length/Å | L–M–L | Bond angle/º |
|---|---|---|---|---|---|---|---|
| Co1—O2 | 2.095 (7) | O39—Co1—O5 | 91.0 (3) | Co2—O8 | 2.178 (7) | O41—Co2—O12 | 91.5 (4) |
| Co1—O3 | 2.117 (7) | O39—Co1—O2 | 94.8 (3) | Co2—O9 | 2.064 (8) | O41—Co2—O9 | 178.5 (4) |
| Co1—O5 | 2.077 (8) | O5—Co1—O2 | 172.0 (3) | Co2—O11 | 2.105 (8) | O12—Co2—O9 | 87.1 (3) |
| Co1—O6 | 2.096 (7) | O39—Co1—O6 | 91.8 (3) | Co2—O12 | 2.062 (7) | O41—Co2—O40 | 90.4 (5) |
| Co1—O38 | 2.118 (9) | O5—Co1—O6 | 80.0 (3) | Co2—O40 | 2.087 (9) | O12—Co2—O40 | 174.6 (4) |
| Co1—O39 | 2.060 (8) | O2—Co1—O6 | 94.4 (3) | Co2—O41 | 2.049 (10) | O9—Co2—O40 | 91.0 (4) |
| | | O39—Co1—O3 | 173.1 (3) | | | O41—Co2—O11 | 87.7 (3) |
| | | O5—Co1—O3 | 94.4 (3) | | | O12—Co2—O11 | 80.2 (3) |
| | | O2—Co1—O3 | 79.4 (3) | | | O9—Co2—O11 | 92.6 (3) |
| | | O6—Co1—O3 | 85.0 (3) | | | O40—Co2—O11 | 94.9 (4) |
| | | O39—Co1—O38 | 88.0 (4) | | | O41—Co2—O8 | 101.0 (3) |
| | | O5—Co1—O38 | 93.5 (3) | | | O12—Co2—O8 | 94.3 (3) |
| | | O2—Co1—O38 | 92.1 (3) | | | O9—Co2—O8 | 78.5 (3) |
| | | O6—Co1—O38 | 173.5 (3) | | | O40—Co2—O8 | 90.3 (4) |
| | | O3—Co1—O38 | 95.8 (3) | | | O11—Co2—O8 | 169.9 (3) |
| **M–L** | **Bond length/Å** | **L–M–L** | **Bond angle/º** | **M–L** | **Bond length/Å** | **L–M–L** | **Bond angle/º** |
| Co3—O14 | 2.033 (8) | O14—Co3—O43 | 93.3 (3) | Co4—O20 | 2.144 (7) | O46—Co4—O21 | 173.3 (4) |
| Co3—O15 | 2.128 (6) | O14—Co3—O18 | 95.2 (3) | Co4—O21 | 2.063 (7) | O46—Co4—O47 | 86.6 (5) |
| Co3—O17 | 2.110 (8) | O43—Co3—O18 | 169.7 (3) | Co4—O23 | 2.119 (8) | O21—Co4—O47 | 86.7 (4) |
| Co3—O18 | 2.080 (7) | O14—Co3—O17 | 173.3 (3) | Co4—O24 | 2.095 (8) | O46—Co4—O24 | 100.8 (3) |
| Co3—O43 | 2.061 (8) | O43—Co3—O17 | 91.6 (3) | Co4—O46 | 2.037 (8) | O21—Co4—O24 | 85.9 (3) |
| Co3—O44— | 2.150 (8) | O18—Co3—O17 | 79.4 (3) | Co4—O47 | 2.093 (9) | O47—Co4—O24 | 171.6 (4) |
| | | O14—Co3—O15 | 80.7 (3) | | | O46—Co4—O23 | 88.3 (3) |
| | | O43—Co3—O15 | 90.5 (3) | | | O21—Co4—O23 | 92.5 (3) |
| | | O18—Co3—O15 | 85.2 (3) | | | O47—Co4—O23 | 97.8 (4) |
| | | O17—Co3—O15 | 94.8 (3) | | | O24—Co4—O23 | 78.7 (3) |
| | | O14—Co3—O44 | 90.7 (3) | | | O46—Co4—O20 | 100.7 (3) |
| | | O43—Co3—O44 | 95.0 (4) | | | O21—Co4—O20 | 79.5 (3) |
| | | O18—Co3—O44 | 90.7 (3) | | | O47—Co4—O20 | 90.5 (3) |
| | | O17—Co3—O44 | 93.4 (3) | | | O24—Co4—O20 | 91.9 (3) |
| | | O15—Co3—O44 | 170.0 (4) | | | O23—Co4—O20 | 168.2 (3) |
| **M–L** | **Bond length/Å** | **L–M–L** | **Bond angle/º** | **M–L** | **Bond length/Å** | **L–M–L** | **Bond angle/º** |
| Co5—O26 | 2.105 (7) | O50—Co5—O29 | 93.3 (3) | Co6—O32 | 2.070 (6) | O51—Co6—O32 | 94.0 (3) |
| Co5—O27 | 2.129 (6) | O50—Co5—O49 | 89.4 (3) | Co6—O33 | 2.156 (7) | O51—Co6—O36 | 169.8 (3) |
| Co5—O29 | 2.072 (6) | O29—Co5—O49 | 90.2 (3) | Co6—O35 | 2.118 (6) | O32—Co6—O36 | 95.0 (3) |

| | | | | | | | |
|---|---|---|---|---|---|---|---|
| Co5—O30 | 2.123 (6) | O50—Co5—O26 | 96.7 (3) | Co6—O36 | 2.092 (7) | O51—Co6—O52 | 90.6 (3) |
| Co5—O49 | 2.100 (6) | O29—Co5—O26 | 169.9 (3) | Co6—O51 | 2.019 (9) | O32—Co6—O52 | 86.5 (3) |
| Co5—O50 | 2.045 (7) | O49—Co5—O26 | 88.9 (3) | Co6—O52 | 2.094 (7) | O36—Co6—O52 | 94.7 (3) |
| | | O50—Co5—O30 | 89.5 (3) | | | O51—Co6—O35 | 92.4 (3) |
| | | O29—Co5—O30 | 80.4 (2) | | | O32—Co6—O35 | 173.7 (3) |
| | | O49—Co5—O30 | 170.5 (3) | | | O36—Co6—O35 | 78.6 (3) |
| | | O26—Co5—O30 | 100.6 (2) | | | O52—Co6—O35 | 93.7 (3) |
| | | O50—Co5—O27 | 171.8 (3) | | | O51—Co6—O33 | 92.3 (3) |
| | | O29—Co5—O27 | 91.0 (2) | | | O32—Co6—O33 | 79.2 (2) |
| | | O49—Co5—O27 | 97.5 (2) | | | O36—Co6—O33 | 84.8 (3) |
| | | O26—Co5—O27 | 79.1 (2) | | | O52—Co6—O33 | 165.6 (3) |
| | | O30—Co5—O27 | 84.4 (2) | | | O35—Co6—O33 | 100.3 (3) |

**Table S3 –** Hydrogen bonds in $\{Co^{II}_6Cu^{II}_6\}$[a,b]

| *D*—H···*A* | *D*—H | H···*A* | *D*···*A* | *D*—H···*A* |
|---|---|---|---|---|
| O42—H42*D*···O37[ii] | 0.90 (1) | 1.84 (1) | 2.708 (14) | 162 (2) |
| O43—H43*C*···O35[ii] | 0.90 (1) | 1.86 (2) | 2.757 (11) | 175 (8) |
| O46—H46*C*···O38[iii] | 0.90 (1) | 2.09 (6) | 2.738 (13) | 128 (6) |
| O47—H47*C*···O25[iv] | 0.91 (1) | 1.82 (1) | 2.633 (9) | 147 (2) |
| O49—H49*D*···O29[v] | 0.90 (1) | 1.98 (3) | 2.746 (9) | 142 (5) |
| O50—H50*D*···O7[i] | 0.90 (1) | 2.07 (6) | 2.704 (9) | 126 (6) |
| O51—H51*C*···O17[vi] | 0.90 (1) | 1.92 (5) | 2.732 (12) | 149 (8) |
| O52—H52*C*···O15[vi] | 0.90 (1) | 1.76 (2) | 2.639 (9) | 165 (6) |
| O40—H40*D*···O31[vii] | 0.90 (1) | 2.35 (3) | 2.948 (11) | 124 (3) |

[a]Symmetry codes: (ii) = *x*+1, *y*-1, *z*; (iii) = *x*+1, *y*-1, *z*+1; (iv) = -*x*+3, -*y*, -*z*+2; (v) = -*x*+2, -*y*+1, -*z*+2; (vi) = *x*-1, *y*+1, *z;* (vii) = -*x*+2, -*y*+1, -*z*+1. [b]Hydrogen bonds involving only the molecules kept in the structure after SQUEEZE technique was applied.

## 3. DFT calculations

DFT type calculations were performed on the full experimental geometry of the $\{Co^{II}_6Cu^{II}_6\}$ nanowheel through the Gaussian 09 package by using the B3LYP functional,[9-11] the quadratic convergence approach and a guess function generated with the fragment tool of the same program.[12] Two all electron basis sets proposed by Ahlrichs *et al.* were used for all atoms, triple- and double-ζ. In both cases, the results are quantitatively similar.[13-14] High-spin cobalt(II) complexes, with a $d^7$ electronic configuration, exhibit a different population of the $t_{2g}$ orbitals, causing the presence of the closed excited states, a feature that makes difficult to find the most stable electronic configuration. This fact is more pronounced when the number of $Co^{II}$ ions increases. To avoid that, we have built $CuCoZn_{10}$ models for each magnetic coupling by replacing the non-involved metal centres by diamagnetic $Zn^{II}$ ions. In such a case, the magnetic coupling for each paramagnetic heterobimetallic pair was obtained from the relative energy of the broken-symmetry (BS) triplet spin state from the high-spin quintet state with parallel local spin moments. More details about the use of the broken-symmetry approach to evaluate the magnetic coupling constants can be found in the literature.[15-19] Because of the low symmetry of the nanowheel (its twelve metal ions being crystallographically independent), twelve magnetic couplings ($J_{i,j}$ running from 1 to 12) were calculated from twelve $CuCoZn_{10}$ models. A polarisable continuum model (PCM) was introduced in the calculations with the parameters corresponding to the acetonitrile.[20]

Additionally, we also performed calculations on the high-spin state of **1**, with $S = 12$, and the corresponding broken-symmetry state with $S = 6$. These calculations were done using Orca 4.1.1.[21] Eight distinct functionals, namely B3LYP,[9-11] BP86,[11,22] PBE0,[23,24] TPSSH,[25,26] BH and HLYP,[27] M06,[28] CAM-B3LYP,[29] and ωB97X-D3[30] were considered. The Ahlrichs[31] def2-SVP basis set was used for all light elements, while Co and Cu were treated with def2-TZVP. To speed up the calculations, the resolution-of-the-identity approximation for the Coulomb integrals (RI-J)[32] and the chain-of-spheres method for exchange integrals (COSX)[33] were applied in combination with the auxiliary def2/J basis set. The calculated energies of the $S = 12$ [*E(HS)*] and $S = 6$ [*E(BS)*] states are shown in Table S5. The BP86 functional, the only pure one in this list, provides the most significant energy gap between these spin states, which agrees with the best accuracy obtained with hybrid functionals, a fact already stated in the past (see refs 18 and 19).

**Table S4.** Relevant structural parameters involved in the different magnetic exchange pathways of the $\{Co^{II}_6Cu^{II}_6\}$ nanowheel together with the more appropriate symmetry for each site and the $J_{i,j}$ values estimated from DFT calculations.

| Coupling | Sites[a] | $d_{M...M}$[b] | $d_{Cu-Ow}$[b] | $h$[c] | Shape analysis for Co/Cu[d,e] | $-J$[f,g] |
|---|---|---|---|---|---|---|
| $J_{1,2}$ | 1,2 | 5.297 | —— | 0.060 | OC-6 (0.586) / SP-4 (1.490) | 71.9 / 75.1 |
| $J_{2,2}$ | 2,2 | 5.340 | —— | | OC-6 (0.629) / SP-4 (1.490) | 77.7 / 78.6 |
| $J_{2,3}$ | 2,3 | 5.303 | 2.331 | 0.153 | OC-6 (0.629) / SPY-5 (0.769) | 61.5 / 62.4 |
| $J_{3,3}$ | 3,3 | 5.321 | 2.331 | | OC-6 (0.640) / SPY-5 (0.769) | 65.2 / 66.9 |
| $J_{3,4}$ | 3,4 | 5.385 | 2.191 | 0.324 (TBPY-5) | OC-6 (0.640) / TBPY-5 (1.663) SPY-5 (2.863) | 58.5 / 59.0 |
| $J_{4,4}$ | 4,4 | 5.360 | 2.191 | 0.158 (SPY-5) | OC-6 (0.895) / TBPY-5 (1.663) SPY-5 (2.863) | 71.1 / 72.5 |
| $J_{4,5}$ | 4,5 | 5.303 | 2.339 | 0.150 | OC-6 (0.895) / SPY-5 (1.194) | 68.0 / 68.7 |
| $J_{5,5}$ | 5,5 | 5.369 | 2.339 | | OC-6 (0.850) / SPY-5 (1.194) | 60.9 / 61.7 |
| $J_{5,6}$ | 5,6 | 5.303 | 2.334 | 0.167 | OC-6 (0.850) / SPY-5 (1.437) | 65.7 / 66.4 |
| $J_{6,6}$ | 6,6 | 5.338 | 2.334 | | OC-6 (1.014) / SPY-5 (1.437) | 69.7 / 70.3 |
| $J_{6,1}$ | 6,1 | 5.388 | 2.262 | 0.188 | OC-6 (1.014) / SPY-5 (1.080) | 60.5 / 61.8 |
| $J_{1,1}$ | 1,1 | 5.355 | 2.262 | | OC-6 (0.586) / SPY-5 (1.080) | 55.4 / 56.1 |

[a]Sites are labelled as $\{Co_i,Cu_j\}$. [b]Values in Å. [c]Values in Å of the shift of the $Cu^{II}$ ion from the mean basal plane. [d]The listed values in parentheses correspond to the deviation between the ideal and real coordination polyhedral. [e]OC-6, $O_h$, octahedron; SP-4, $D_{4h}$, square; SPY-5, $C_{4v}$, square pyramid; TBPY-5, $D_{3h}$, trigonal bipyramid. [f]Values in $cm^{-1}$. [g]Values using the SV/TZV basis sets.

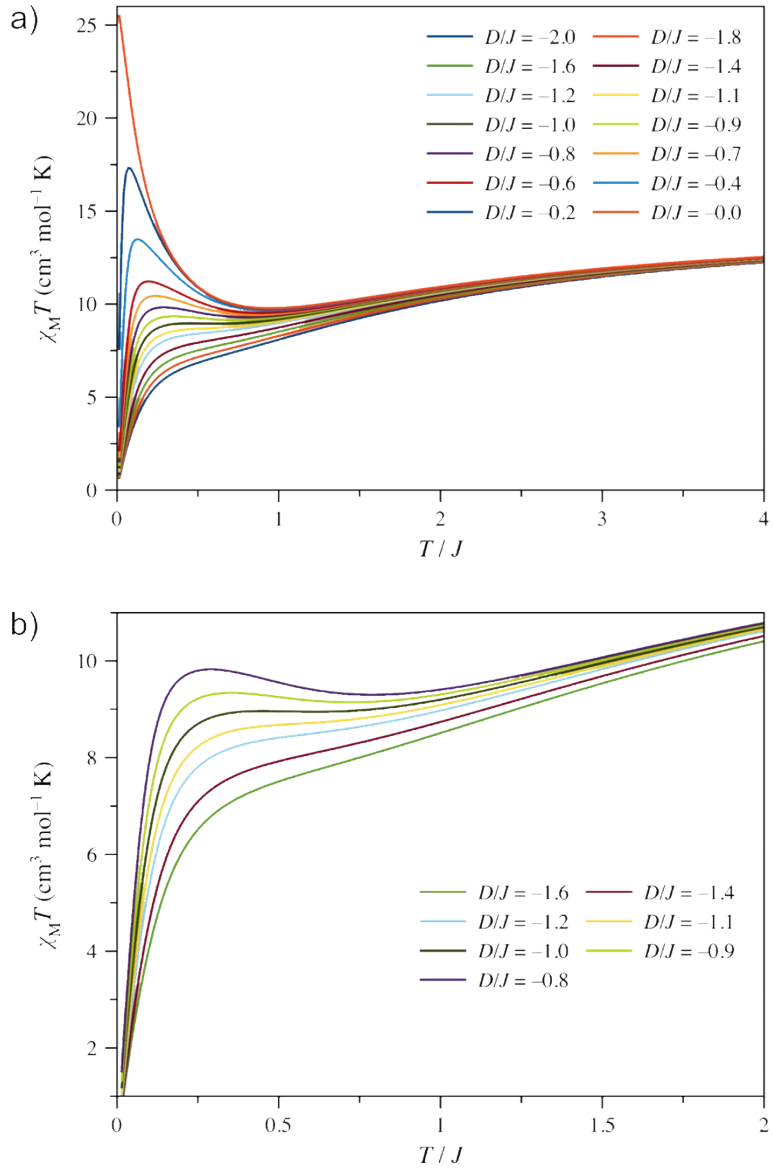


**Figure S5.** Reduced $\chi_M T$ *vs*. *T/J* plots as a function of the *D/J* quotient in the ranges (a) 0.0 to –2.0 and (b) –0.8 to –1.6. All curves were simulated considering $J = -50$ cm$^{-1}$.

**Table S5.** Electronic energies (in hartrees) of the high-spin state ($S$ = 12) [*E(HS)*] and broken symmetry ($S$ = 6) [*E(BS)*] states of **1** obtained using distinct density functionals.

| **Functional** | ***E(HS)*** | ***E(BS)*** | ***E(HS)-E(BS) ($cm^{-1}$)*** |
|---|---|---|---|
| ωB97X-D3 | -26954.882090 | -26954.886620 | 994.3 |
| CAM-B3LYP | -26954.181722 | -26954.186319 | 1008.9 |
| PBE0 | -26944.354010 | -26944.359789 | 1268.4 |
| B3LYP | -26951.224586 | -26951.232100 | 1649.1 |
| M06 | -26951.182742 | -26951.190662 | 1738.1 |
| TPSSH | -26957.320006 | -26957.329629 | 2111.8 |
| BHandHLYP | -26951.522662 | -26951.533645 | 2410.2 |
| BP86 | -26959.758530 | -26959.779675 | 4640.4 |

## 4. EPR measurements

The EPR spectroscopic properties of the $\{Co^{II}_6Cu^{II}_6\}$ nanowheel were investigated in the solid-state. The measurements at X-band (9.38 GHz) were carried out using a Bruker ELEXSYS E580 CW EPR spectrometer equipped with an Oxford Instruments helium cryostat (ESR900) and a MercuryiTC temperature controller. The powder EPR spectra are silent down to 25 K. Below this temperature, an intense signal with apparent axial symmetry and a zero crossing at $g$ = 0.57 appears, revealing the unique electronic properties of the heterobimetallic complex (see Figure S6). Signals in the typical region of isolated cobalt(II) or copper(II) ions in the $g$ value range of 2 - 4 are virtually absent.[34] The EPR data is consistent with a non-Kramers system with a large zero-field splitting resulting from the coupling of the half-integer spins of copper(II) and cobalt(II).

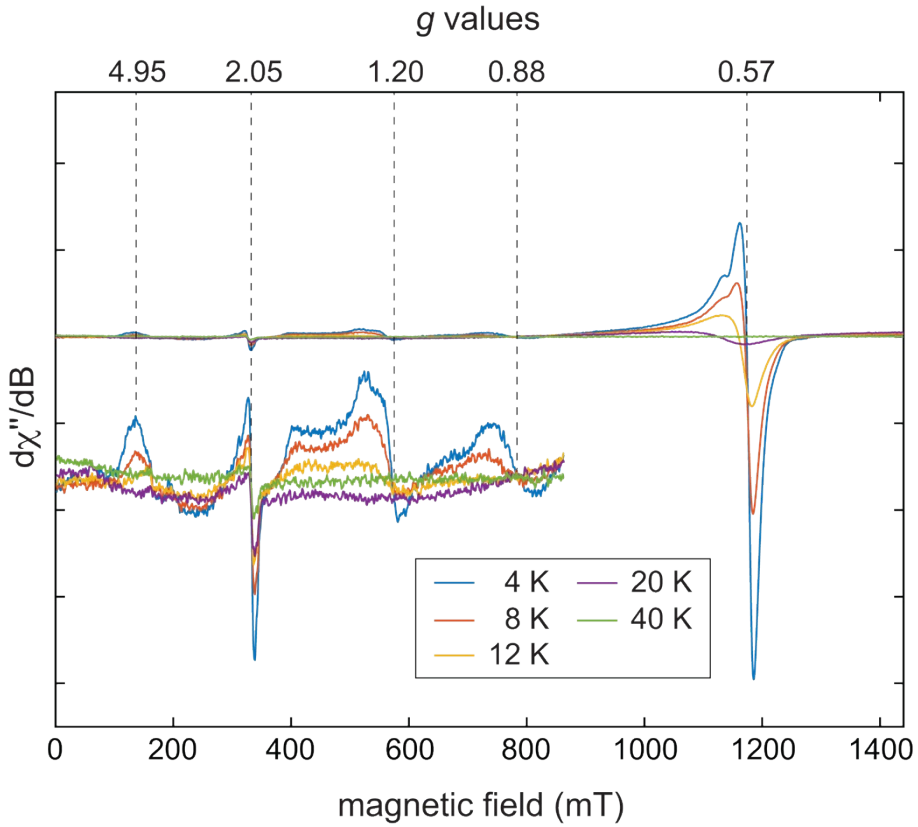


**Figure S6.** Variable temperature X-band EPR spectra of the $\{Co^{II}_6Cu^{II}_6\}$ nanowheel between 4.0 and 40 K. The inset shows an expanded view of the low-field part of the spectrum. The signal around a $g$ value of 2.05 could be due to trace amounts of some uncoupled mononuclear copper(II) ions.

## 5. References


1 W. D. do Pim, W. X. C. Oliveira, M. A. Ribeiro, É. N. de Faria, I. F. Teixeira, H. O. Stumpf, R. M. Lago, C. L. M. Pereira, C. B. Pinheiro, J. C. D. Figueiredo-Júnior, W. C. Nunes, P. P. de Souza, E. F. Pedroso, M. Castellano, J. Cano, M. Julve, *Chem. Commun.,* 2013, **49**, 10778.

2 G. A. Bain, J. F. Berry, *J. Chem. Educ.,* 2008, **85**, 532.

3 E. CrysAlisPRO. Rigaku Oxford Diffraction: Yarnton, Oxfordshire, 2018.

4 L. Palatinus, G. Chapuis, *J. Appl. Crystallogr.,* 2007, **40**, 786–790.

5 G. M. Sheldrick, *Acta Crystallogr. Sect. C Struct. Chem.,* 2015, **71**, 3–8.

6 C. K. Johnson, *Crystallographic Computing*, Munksgaard, Copenhagen, 1970.

7 A. L. Spek, *Acta Crystallogr. Sect. C,* 2015, **71**, 9–18.

8 C. F. Macrae, I. Sovago, S. J. Cottrell, P. T. A. Galek, P. McCabe, E. Pidcock, M. Platings, G. P. Shields, J. S. Stevens, M. Towler, P. A. Wood, *J. Appl. Crystallogr.* 2020, **53**, 226–235.

9 A. D. Becke, *Phys. Rev. A,* 1998, **38**, 3098-3100.

10 C. Lee, W. Yang, R. G. Parr, *Phys. Rev. B,* 1988, **37**, 785–789.

11 A. D. Becke, *J. Chem. Phys.,* 1993, **98**, 5648–5652.

12 M. J. Frisch, G. W. Trucks, H. B. Schlegel, G. E. Scuseria, M. A. Robb, J. R. Cheeseman, G. Scalmani, V. Barone, B. Mennucci, G. A. Petersson, H. Nakatsuji, M. Caricato, X. Li, H. P. Hratchian, A. F. Izmaylov, J. Bloino, G. Zheng, J. L. Sonnenberg, M. Hada, M. Ehara, K. Toyota, R. Fukuda, J. Hasegawa, M. Ishida, T. Nakajima, Y. Honda, O. Kitao, H. Nakai, T. Vreven, J. A. Montgomery Jr., J. E. Peralta, F. Ogliaro, M. Bearpark, J. J. Heyd, E. Brothers, K. N. Kudin, V. N. Staroverov, R. Kobayashi, J. Normand, K. Raghavachari, A. Rendell, J. C. Burant, S. S. Iyengar, J. Tomasi, M. Cossi, N. Rega, J. M. Millam, M. Klene, J. E. Knox, J. B. Cross, V. Bakken, C. Adamo, J. Jaramillo, R. Gomperts, R. E. Stratmann, O. Yazyev, A. J. Austin, R. Cammi, C. Pomelli, J. W. Ochterski, R. L. Martin, K. Morokuma, V. G. Zakrzewski, G. A. Voth, P. Salvador, J. J. Dannenberg, S. Dapprich, A. D. Daniels, Ö. Farkas, J. B. Foresman, J. V Ortiz, J. Cioslowski, D. J. Fox, *Gaussian 09,* Gaussian, Inc., Wallingford CT, 2009.

13 A. Schäfer, H. Horn, R. Ahlrichs, *J. Chem. Phys.,* 1992, **97**, 2571–2577.

14 A. Schäfer, C. Huber, R. Ahlrichs, *J. Chem. Phys.,* 1994, **100**, 5829–5835

15 E. Ruiz, A. Rodríguez-Fortea, J. Cano, S. Alvarez, P. Alemany, *J. Comp. Chem.* 2003, **24**, 982–989.

16 E. Ruiz, J. Cano, S. Alvarez, P. Alemany, *J. Am. Chem. Soc.,* 1998, **120**, 11122–11129.

17 E. Ruiz, P. Alemany, S. Alvarez, J. Cano, *J. Am. Chem. Soc.,* 1997, **119**, 1297–1303.

18 E. Ruiz, J. Cano, S. Alvarez, P. Alemany, *J. Comput. Chem.,* 1999, **20**, 1391–1400.

19 E. Ruiz, S. Alvarez, J. Cano, V. Polo, *J. Chem. Phys.,* 2005, **123**, 164110.

20 J. Tomasi, B. Mennucci, R. Cammi, *Chem. Rev.*, 2005, **105**, 2999-3093.

21 F. Neese, *Wiley Interdiscip. Rev. Comput. Mol. Sci.,* 2012, **2**, 73–78.

22 J. P. Perdew, *Phys. Rev. B,* 1986, **33**, 8822–8824.

23 M. Ernzerhof, G. E. Scuseria, *J. Chem. Phys.,* 1999, **110**, 5029–5036.

24 C. Adamo, V. Barone, *J. Chem. Phys.,* 1999, **110**, 6158–6170.

25 J. Tao, J. P. Perdew, V. N. Staroverov, G. E. Scuseria, *Phys. Rev. Lett.,* 2003, **91**, 146401.

26 V. N. Staroverov, G. E. Scuseria, J. Tao, J. P. Perdew, *J. Chem. Phys.,* 2003, **119**, 12129–12137.

27 A. D. Becke, *J. Chem. Phys.,* 1993, **98**, 1372–1377.

28 Y. Zhao, D. G. Truhlar, *Theor. Chem. Acc.,* 2008, **120**, 215–241.

29 T. Yanai, D. P. Tew, N. C. Handy, *Chem. Phys. Lett.,* 2004, **393**, 51–57.

30 Y.-S. Lin, G.-D. Li, S.-P. Mao, J.-D. Chai, *J. Chem. Theory Comput.,* 2013, **9**, 263–272.

31 F. Weigend, R. Ahlrichs, *Phys. Chem. Chem. Phys.,* 2005, **7**, 3297–3305.

32 F. Neese, *J. Comput. Chem.,* 2003, **24**, 1740–1747.

33 F. Neese, F. Wennmohs, A. Hansen, U. Becker, *Chem. Phys.,* 2009, **356**, 98–109.

34 F. E. Mabbs, Collison, D. Collison, *Electron Paramagnetic Resonance of d Transition Metal Compounds (Studies in Inorganic Chemistry)*, Elsevier Science, Amsterdam, 1992.